

Population genetics of swamp eel in the Yangtze River: comparative analyses between mitochondrial and microsatellite data provide novel insights

Huaxing Zhou^{Equal first author, 1}, Yuting Hu^{Equal first author, 1}, He Jiang^{Corresp., 1}, Guoqing Duan¹, Jun Ling¹, Tingshuang Pan¹, Xiaolei Chen¹, Huan Wang¹

¹ Anhui Key Laboratory of Aquaculture and Stock Enhancement, Fisheries Research Institution, Anhui Academy of Agricultural Sciences, Hefei, China

Corresponding Author: He Jiang
Email address: kenc7c7c7@126.com

The swamp eel (*Monopterus albus*) is a typical sex reversal fish with the high economic value. Several phylogeographic studies have been performed using various markers but comparative research between mitochondrial and nuclear markers is rare. Here, a fine-scale study was performed across six sites along the Yangtze River including three sites on the main stem and three sites from tributaries. A total of 180 swamp eel individuals were collected. Genetic structure and demographic history were explored using data from two mitochondrial genes and eight microsatellite loci. The results revealed the samples from tributary sites formed three separate clades which contained site-specific lineages. Geographic isolation and the habitat patchiness caused by seasonal cutoff were inferred to be the reasons for this differentiation. Strong gene flow was detected among the sites along the main stem. Rapid flow of the river main stem may provide the dynamic for the migration of swamp eel. Interestingly, the comparative analyses between the two marker types was discordant. Mitochondrial results suggested samples from three tributary sites were highly differentiated. However, microsatellite analyses indicated the tributary samples were moderately differentiated. We conclude this discordance is mainly caused by the unique life history of sex reversal fish. Our study provides novel insights regarding the population genetics of sex reversal fish.

1 **Population genetics of swamp eel in the Yangtze River: comparative analyses**
2 **between mitochondrial and microsatellite data provide novel insights**

3

4 **Huaxing Zhou¹①, Yuting Hu¹①, He Jiang¹✉, Guoqing Duan¹, Jun Ling¹, Tingshuang**
5 **Pan¹, Xiaolei Chen¹, Huan Wang¹**

6

7 **¹ Anhui Key Laboratory of Aquaculture and Stock Enhancement, Fisheries**
8 **Research Institution, Anhui Academy of Agricultural Sciences, Hefei, China**

9

10 ✉: **Corresponding author:**

11 **He Jiang**

12 **The Nongkenan road, Hefei, Anhui, 230031, China**

13 **Email address: kenc7c7c7@126.com**

14

15 **①: These authors contributed equally to this work**

17 **Abstract**

18 The swamp eel (*Monopterus albus*) is a typical sex reversal fish with the high
19 economic value. Several phylogeographic studies have been performed using various
20 markers but comparative research between mitochondrial and nuclear markers is rare.
21 Here, a fine-scale study was performed across six sites along the Yangtze River including
22 three sites on the main stem and three sites from tributaries. A total of 180 swamp eel
23 individuals were collected. Genetic structure and demographic history were explored
24 using data from two mitochondrial genes and eight microsatellite loci. The results
25 revealed the samples from tributary sites formed three separate clades which contained
26 site-specific lineages. Geographic isolation and the habitat patchiness caused by
27 seasonal cutoff were inferred to be the reasons for this differentiation. Strong gene flow
28 was detected among the sites along the main stem. Rapid flow of the river main stem
29 may provide the dynamic for the migration of swamp eel. Interestingly, the comparative
30 analyses between the two marker types was discordant. Mitochondrial results suggested
31 samples from three tributary sites were highly differentiated. However, microsatellite
32 analyses indicated the tributary samples were moderately differentiated. We conclude
33 this discordance is mainly cause by the unique life history of sex reversal fish. Our study
34 provides novel insights regarding the population genetics of sex reversal fish.

35 **Keywords:** *Monopterus albus*; Sex reversal; Population genetics; Mitochondrial and
36 nuclear markers

38 Introduction

39 The swamp eel (*Monopterus albus*) is a typical sex reversal fish, belonging to the
40 family Synbranchidae, which usually inhabits swamps, ponds and rice fields (Nelson,
41 Grande & Wilson, 2016). Due to its high nutrition value and good taste, the swamp eel is
42 used as a significant aquatic food in China. In 2018, 0.32 million tons of swamp eel were
43 produced by Chinese aquaculture (data from The Ministry of Agriculture of China, 2019).

44 With the development of swamp eel farming, population genetic research of the wild
45 eel became a hot topic, which has been used to guide the genetic breeding and swamp
46 eel aquaculture. Several studies have used different markers including microsatellites,
47 mitochondrial sequences and Inter-simple sequence repeats (ISSR) to explore swamp
48 eel population genetics (Lei et al., 2012; Li et al., 2013; Liang et al., 2016). Previous
49 studies suggested a rapid decrease of wild swamp eel caused by the large use of
50 pesticides and over exploitation (Li et al., 2013; Liang et al., 2016). Cultured populations
51 were genetically less diverse than wild populations. Due to the escape from farm, the
52 populations of wild swamp eel was suffering from mix of variety and degeneration of
53 genetic characterization (Li et al., 2013). Thus, further researches of population genetics
54 and dynamics are necessary to protect the wild swamp eel.

55 *Monopterus albus* is a sex reversal fish with a unique life history (Liu, 1944; Mazzoni
56 et al., 2018; Qu, 2018). It starts the reproductive cycle as a functional female. During 1 to
57 1.5 years of age, swamp eel obtains well-developed ova. After spawning, the swamp eel's
58 sex is reversed from female to male. The intersexes appear in two-year-old swamp eel.
59 Then it lives as male without sex reversal (Liem, 1963). Generally, swamp eel can live to
60 6-8 years. Mitochondrial DNA is maternal inherited. For this reason, the inheritance
61 patterns of protogynous species differs to that of fishes that do not practice sex reversal.
62 Therefore, it may be important to include both nuclear and mitochondrial markers to
63 explore the population genetic structure of sex reversal fish.

64 This fine-scale study was performed across six sites along the Yangtze River
65 including three sites on the main stem and three sites from tributaries. Subsequently, the

66 genetic structure of these six sampling sites was explored, using sequence from two
67 mitochondrial genes and eight microsatellite loci. Here, we show how different types of
68 molecular markers can provide new insights regarding the population genetics of sex
69 reversal fish.

70 **Materials & Methods**

71 **Ethics statement and Sample collection**

72 Procedures involving animals and their care were approved by the Animal Care and
73 Use Committee of Anhui Academy of Agricultural Sciences under approval number
74 201003076. Field experiments were approved by Fisheries Bureau of Anhui (project
75 number: FB/AH 2017-10).

76 A total of 180 eel individuals were collected using net from six sites along the Anhui
77 basin of the Yangtze River (Table S1). Sampling sites from tributaries of the Yangtze
78 River included Dang Tu (DT), Fan Chang (FC) and Huai Ning (HN); sampling sites from
79 the main stem of the Yangtze River included Wu Wei (WW), Gui Chi (GC) and Wang
80 Jiang (WJ) (Fig. 1).

81 **DNA extraction and Marker genotyping**

82 Total genomic DNA was extracted from muscle tissue using a standard
83 phenol/chloroform procedure via proteinase K digestion (Sambrook, Fritsch & Maniatis,
84 1989), and then kept at -20°C for PCR amplification.

85 The mitochondrial cytochrome c oxidase subunit I (*COI*) gene and cytochrome b (*Cyt*
86 *b*) gene were chosen. Two pairs of primers were designed here for the amplification
87 (Table S2). PCR were conducted in 50 µL reaction mixtures containing 200 ng template
88 DNA, 5 µL 10 × buffer (TaKaRa, Dalian, China), 4 µL MgCl₂ (2.5 mol/L), 3 µL dNTP (2.5
89 m mol/L), 2 µL of each primer (5 µmol/L), and 1 U Taq DNA polymerase (5 U/µL,
90 TaKaRa). PCR conditions were as follows: initial denaturation (95°C, 1 min), then 35
91 cycles of denaturation (94°C, 50 s), primer annealing (55°C, 45 s), and elongation (72°C,
92 1 min) and a final extension (72°C, 10 min). All fragments were sequenced in both

93 directions with an ABI3730 automated sequencer (Invitrogen Biotechnology Co., Ltd,
94 USA).

95 Eight unlinked polymorphic microsatellite loci were selected from previous studies
96 (Table S1) (Lei et al., 2012; Li et al., 2007; Zhuo et al., 2011). PCR were conducted in 50
97 μL reaction mixtures containing 200 ng template DNA, 5 μL 10 \times buffer (TaKaRa, Dalian,
98 China), 4 μL MgCl_2 (2.5 mol/L), 2.5 μL dNTP (2.5 m mol/LM), 2 μL of each primer (5
99 $\mu\text{mol/L}$), and 1 U Taq DNA polymerase (25 U/ μL , TaKaRa). PCR conditions were as
100 follows: initial denaturation (95°C, 5 min), then 32 cycles of denaturation (94°C, 30 s),
101 primer annealing (57°C, 60 s), and elongation (72°C, 90 s) and a final extension (72°C, 5
102 min). Genotype was detected by ABIPRISM 3730.

103 **Data analyses**

104 **Mitochondrial sequence**

105 Sequences were assembled by DNASTAR Lasergene package. Subsequent
106 homologous alignment was performed by Mafft v.7 online program
107 (<https://mafft.cbrc.jp/alignment/software/>) (Katoh, Rozewicki & Yamada, 2017).

108 Haplotype and nucleotide diversity were estimated using DNAsp V.6 (Rozas et al.,
109 2017). A parsimony network was constructed using Median Joining (MJ) in NETWORK
110 v.5.0 (Bandelt, Forster & Röhl, 1999). Analysis of Molecular Variance (AMOVA) was
111 performed using Arlequin v.3.11 (Excoffier, Laval & Schneider, 2005). Genetic variation
112 within and among sampling sites was assessed. Pairwise F_{st} was estimated in order to
113 evaluate the levels of population differentiation (Slatkin and Barton, 1989) and the P
114 values were corrected using multiple testing.

115 The demographic history was explored using three approaches, e.g., neutrality tests,
116 mismatch distribution and Bayesian Skyline Plots (BSP) analyses. Tajima's D (Tajima,
117 1989) and Fu's F_s (Fu, 1997) values were calculated using DNAsp V.6. Mismatch
118 distribution analyses were performed using Arlequin v.3.11 (Rogers & Harpending, 1992).
119 The expansion time was calculated by the τ value with the equation $\tau = 2\mu t$, where μ
120 represents the nucleotide mutation rate and t represents the estimated expansion time.

121 BSP analysis was performed using Beast v1.10.4 (Suchard et al., 2018) under an
122 uncorrelated relaxed clock mode for 5×10^7 generations.

123 **Microsatellites data**

124 The results of 8 microsatellites loci were read using GeneMarker (Holland & Parson,
125 2011) and reformatted using Convert v.1.31 (Glaubitz, 2004). Hardy-Weinberg
126 equilibrium (HWE) test was performed using Popgene v 1.32 (Yeh et al., 1999). Expected
127 and observed heterozygosity were calculated with Arlequin v.3.11 (Rogers & Harpending,
128 1992). AMOVA was implemented with Arlequin. Pairwise F_{st} was computed based on
129 Slatkin's method (Slatkin & Barton, 1989). The geographical and genetic distance
130 between sample sites was measured by GPS and Popgene v 1.32, respectively. The
131 correlation between geographical and genetic distance was analyzed using Pcord v 5
132 (Grandin, 2006).

133 Population structure was estimated using an MCMC (Markov Chain Monte Carlo)
134 algorithm as implemented in Structure v.2.3.3 (Hubisz et al., 2009). The number of
135 clusters (K) was calculated under 1×10^6 iterations with 10 replications and the optimal
136 number of K was deduced by Structure Harvester Web v.0.6.94 (Evanno, Regnaut &
137 Goudet, 2005; Earl, 2012).

138 **Results**

139 **Mitochondrial genes**

140 A total of 1752 bp of mitochondrial sequence (*COI* 665 bp, Accession number:
141 MN097948 - MN098127; *Cyt b* 1087 bp, Accession number: MN098128 - MN098307)
142 was obtained for analyses. The contents of the bases A, T, G and C were 24.6%, 29.3%,
143 14.6% and 31.5% respectively, which showed obvious anti-G bias (Saccone et al., 1999).

144 The 180 mitochondrial sequences corresponded to 86 distinct haplotypes (Table 1).
145 All haplotypes were divided into four clades based on MJ method (Fig. 2). Clade A was
146 the largest one which contained samples from five sampling sites. Haplotype 5 (H-5) had
147 the largest number of shared individuals, and its central placement in the network
148 suggests that this is the ancestral haplotype. The other three clades were separated by

149 13, 47, 24 mutational steps, respectively. Clade B only contained samples from the HN
150 sampling site. Clade C and D mainly consisted of FC and DT samples, respectively.

151 Haplotype diversity ranged from 0.6620 to 0.9793 and nucleotide diversity ranged
152 from 0.0017 to 0.0148 based on mitochondrial sequence (Table 1). The results of AMOVA
153 showed that genetic variation among sampling sites (71.23%, $P < 0.001$) were much
154 higher than the variation within the sampling sites (28.77%, $P < 0.001$) (Table 2a).
155 Subsequent F_{st} values further confirmed this result. Strong gene flow was detected
156 between the main stem sampling sites ($F_{st} = 0.0242$ between GC and WW, $F_{st} = 0.0286$
157 between WJ and WW, $F_{st} = 0.0305$ between WJ and GC, see Table 3a). And high
158 differentiation was revealed between the tributary sampling sites ($F_{st} = 0.3069 - 0.9431$)
159 (Table 3a). Fu's F_s and Tajima's D tests of main stem samples were significant ($P < 0.01$)
160 but negative. No explicit expansion or decline were revealed for the tributary samples and
161 the Fu's F_s and Tajima's D values except the Tajima's D of FC were not significant (Table
162 4). Mismatch distribution analysis revealed similar results. The values of sum of squares
163 deviations (SSD) for samples from main stem and DT were not significant ($P > 0.05$),
164 indicating that sudden expansion could not be rejected (Table 4). The BSP analysis
165 suggested the main stem samples had suffered effective population size decline (Fig. 3).
166 Subsequent expansion time was indicated roughly as 0.46 MYA.

167 **Microsatellite loci**

168 The eight microsatellite loci amplified unambiguous and repeatable products in the
169 size range expected. All loci were in Hardy-Weinberg equilibrium ($P > 0.05$). High genetic
170 diversity was also supported by microsatellite data. Expected and observed
171 heterozygosity for the six sampling sites were 0.8052 - 0.8749 and 0.5958 - 0.7917,
172 respectively (Table 1).

173 Structure results suggested the highest posterior probability for $K=4$ (Fig. S1). The
174 ΔK method revealed four potential genetic clusters, aligning with the three tributaries and
175 all the main stem sites together. Samples from main stem showed high levels of genetic
176 admixture (Fig. 4).

177 AMOVA was performed using the microsatellite data and suggested that genetic
178 variation was mainly within sampling sites (94.65%, $P < 0.001$), opposite to the results
179 from mitochondrial data (Table 2b). F_{st} values suggested low levels of differentiation (F_{st}
180 = 0.0005 - 0.0982) (Table 3b).

181 The correlation between genetic and geographic matrixes was assessed using
182 Mantel test (Table S3). The results suggested a significant correlation between them ($r =$
183 0.8791, $P = 0.004$) (Fig. 5).

184 Discussion

185 Population genetics of swamp eel

186 High levels of genetic diversity were found across sampling sites at both
187 mitochondrial and microsatellite markers. The genetic diversity level of this study except
188 FC sample site was higher than previous study in the same basin ($Hd = 0.708$ and $Pi =$
189 0.002 based on mitochondrial D-loop sequences) (Liang et al., 2016). The genetic
190 diversity of FC samples was the lowest ($Hd = 0.6620$, $Pi = 0.0017$). The significant
191 differentiation of three tributary sampling sites was revealed by the population genetic
192 analyses ($F_{st} > 0.25$). The haplotype network and structure results suggested the tributary
193 samples formed three separate clades which contained site-specific lineages. Significant
194 correlation between genetic and geographic distance was detected. Interestingly, strong
195 gene flow was detected among the main stem sampling sites and the expansion of main
196 stem samples was detected.

197 It is well known that the swamp eel is a burrowing fish whose fins are vestigial or
198 absent (Nelson, Grande & Wilson, 2016). Compared with most fishes, the swimming
199 ability of eel is weak. Thus, we were curious about the reasons for this long-distance gene
200 flow among main stem sampling sites. The flow rate of main stem in Anhui basin range
201 up to 1.0 m/s (Guo & Xia, 2007). Rapid flow provides the dynamic for the migration of
202 swamp eel. The eggs and juvenile fishes can slip downstream to the farther places.
203 However, due to the flat stream gradient and curved channel, tributary flow becomes
204 slower (Zhang, Li & Jiang, 2008) and long-distance migration is difficult for swamp eel.

205 We propose that geographic isolation and the habitat patchiness caused by seasonal
206 cutoff are the reasons for the differentiation between tributary samples. The tributary of
207 FC site was much more isolated from the main stem. It connected to the main stem during
208 the wet season and isolated during the dry season. Long-term isolation from the main
209 stem may cause the low genetic diversity of FC samples.

210 **Comparative analyses between mitochondrial and microsatellite data**

211 Analyses of nuclear and mitochondrial markers revealed discordant population
212 structure in tributary samples. Based on mitochondrial data, genetic variation was mainly
213 found among sampling sites. Samples between the tributary sites were highly
214 differentiated ($F_{st} > 0.25$) and represented three monophyletic clades. However,
215 microsatellite analyses suggest that the majority of genetic variation is within these
216 sampling sites; samples between the tributary sites were moderately differentiated (0.05
217 $< F_{st} < 0.15$). Mean F_{st} values of tributary samples based on mitochondrial and
218 microsatellite data were 0.6777 and 0.0679, respectively. Considering the different
219 mutation rates of these two genomes, we corrected the mitochondrial F_{st} using the
220 equation, $F_{st}(\text{nuc}) = F_{st}(\text{mt})/[4-3 F_{st}(\text{mt})]$ (Brito, 2007). Even so, corrected mitochondrial
221 F_{st} value (0.3445) was still five times higher than the F_{st} (0.0679) estimated with
222 microsatellite data. Conversely, the mean F_{st} values of main stem samples based on
223 mitochondrial genes and microsatellite data were 0.0278 and 0.0037, respectively. After
224 correction, both mitochondrial and microsatellite F_{st} reflected no differentiation among
225 sampling sites of main stem.

226 Our study provided an interesting pattern of discordance between markers in the tributary
227 samples as compared to consistent results between markers when considering main
228 stem samples. According to previous studies, sex-biased dispersal, genetic admixture
229 and lineage sorting may be the potential reasons for the discordance caused by different
230 molecular markers (Funk and Omland, 2003; Qu et al., 2012; Yang et al., 2016; Zarza et
231 al., 2011). Considering the sex reversal in this species, we inferred the unique life history
232 of the swamp eel contributed to this discordance, which was different from previous

233 studies. Initially, the swamp eel is female and provides both mitochondrial and nuclear
234 DNA to the population genetic pool. After spawning, the swamp eel becomes male. Due
235 to mitochondrial maternal inheritance, male swamp eels only provide nuclear DNA to the
236 population genetic pool (Fig. 6). As mentioned above, male stage is much longer than
237 female stage in the whole life of swamp eel that cause different genetic frequencies
238 between mitochondrial and nuclear data. The five-fold difference between mitochondrial
239 and nuclear F_{st} values in tributary samples also confirmed this view. Consistent results
240 between markers in main stem samples indicated extensive gene flow could reduce the
241 effect of the sex reversal life history on the population genetic structure.

242 **Conclusions**

243 Our study used two data sets, mitochondrial DNA and microsatellites, to explore the
244 demography, genetic variation and population structure of swamp eels. Compare with
245 previous studies, high levels of genetic diversity suggest that swamp eels are an
246 abundant resource in the Anhui basin and have potential commercial value. Samples from
247 each tributary site in this study should be treated as an independent genetic unit. The
248 unique sex reversal life history of the swamp eel may be significant factors affecting the
249 population genetic structure and may generate the discordance we found between
250 different molecular markers. Our study provides novel insights regarding the population
251 genetics of sex reversal fish.

252

253 **Acknowledge**

254 We thank Prof. Lee Rollins, Adomas Ragauskas and Joana Robalo for their
255 constructive comments.

257 **References**

- 258 Bandelt HJ, Forster P, Röhl A. 1999. Median-joining networks for inferring intraspecific
259 phylogenies. *Molecular biology and evolution* 16: 37-48.
- 260 Brito PH. 2007. Contrasting patterns of mitochondrial and microsatellite genetic structure
261 among Western European populations of tawny owls (*Strix aluco*). *Molecular ecology*
262 16: 3423-3437.
- 263 Earl DA. 2012. STRUCTURE HARVESTER: a website and program for visualizing
264 STRUCTURE output and implementing the Evanno method. *Conservation genetics*
265 *resources* 4: 359-361.
- 266 Evanno G, Regnaut S, Goudet J. 2005. Detecting the number of clusters of individuals
267 using the software STRUCTURE: a simulation study. *Molecular ecology* 14: 2611-
268 2620.
- 269 Excoffier L, Laval G, Schneider S. 2005. Arlequin (version 3.0): an integrated software
270 package for population genetics data analysis. *Evolutionary bioinformatics* 1: 47-50.
- 271 Fu YX. 1997. Statistical tests of neutrality of mutations against population growth,
272 hitchhiking and background selection. *Genetics* 147: 915-925.
- 273 Funk DJ, Omland KE. 2003. Species-level paraphyly and polyphyly: frequency, causes,
274 and consequences, with insights from animal mitochondrial DNA. *Annual Review of*
275 *Ecology, Evolution, and Systematics* 34: 397-423.
- 276 Glaubitz JC. 2004. Convert: a user - friendly program to reformat diploid genotypic data
277 for commonly used population genetic software packages. *Molecular Ecology*
278 *Notes* 4: 309-310.
- 279 Grandin U. 2006. PC - ORD version 5: A user - friendly toolbox for ecologists. *Journal of*
280 *Vegetation Science* 17: 843-844.
- 281 Guo WX, Xia ZQ. 2007. Study on ecological flow in the middle and lower reaches of the
282 Yangtze River. *Journal of Hydraulic Engineering* 10: 618-623.
- 283 Holland MM, Parson W. 2011. GeneMarker® HID: A reliable software tool for the analysis
284 of forensic STR data. *Journal of forensic sciences* 56: 29-35.

- 285 Hubisz MJ, Falush D, Stephens M, Pritchard JK. 2009. Inferring weak population structure
286 with the assistance of sample group information. *Molecular ecology resources* 9:
287 1322-1332.
- 288 Katoh K, Rozewicki J, Yamada KD. 2017. MAFFT online service: multiple sequence
289 alignment, interactive sequence choice and visualization. *Briefings in bioinformatics*.
- 290 Lei L, Feng L, Jian TR, Yue GH. 2012. Characterization and multiplex genotyping of novel
291 microsatellites from Asian swamp eel, *Monopterus albus*. *Conservation genetics*
292 *resources* 4: 363-365.
- 293 Li W, Liao X, Yu X, Cheng L, Tong J. 2007. Isolation and characterization of polymorphic
294 microsatellites in a sex-reversal fish, rice field eel (*Monopterus albus*). *Molecular*
295 *ecology notes* 7: 705-707.
- 296 Li W, Sun WX, Fan J, Zhang CC. 2013. Genetic diversity of wild and cultured swamp eel
297 (*Monopterus albus*) populations from central China revealed by ISSR markers.
298 *Biologia* 68: 727-732.
- 299 Liang H, Guo S, Li Z, Luo X, Zou G. 2016. Assessment of genetic diversity and population
300 structure of swamp eel *Monopterus albus* in China. *Biochemical systematics and*
301 *ecology* 68: 81-87.
- 302 Liem KF. 1963. Sex reversal as a natural process in the synbranchiform fish *Monopterus*
303 *albus*. *Copeia* 2: 303-312.
- 304 Liu CK. 1944. Rudimentary hermaphroditism in the symbranchoid eel, *Monopterus*
305 *favanensis*. *Sinensia* 15: 1-18.
- 306 Mazzoni T, Lo Nostro F, Antoneli F, Quagio-Grassiotto I. 2018. Action of the
307 Metalloproteinases in Gonadal Remodeling during Sex Reversal in the Sequential
308 Hermaphroditism of the Teleostei Fish *Synbranchus marmoratus*
309 (Synbranchiformes: Synbranchidae). *Cells* 7: 34.
- 310 Nelson JS, Grande TC, Wilson MV. 2016. Fishes of the world. John Wiley & Sons Press.
- 311 Qu XC. 2018. Sex determination and control in eels. In: *Sex Control in Aquaculture*. John
312 Wiley & Sons Press. 775-792.

- 313 Qu Y, Zhang R, Quan Q, Song G, Li SH, Lei F. 2012. Incomplete lineage sorting or
314 secondary admixture: disentangling historical divergence from recent gene flow in
315 the Vinous-throated parrotbill (*Paradoxornis webbianus*). *Molecular ecology* 21:
316 6117-6133.
- 317 Rogers AR, Harpending H. 1992. Population growth makes waves in the distribution of
318 pairwise genetic differences. *Molecular biology and evolution* 9: 552-569.
- 319 Rozas J, Ferrer-Mata A, Sánchez-DelBarrio JC, Guirao-Rico S, Librado P, Ramos-Onsins
320 SE, Sánchez-Gracia A. 2017. DnaSP 6: DNA sequence polymorphism analysis of
321 large data sets. *Molecular biology and evolution* 34: 3299-3302.
- 322 Saccone C, De Giorgi C, Gissi C, Pesole G, Reyes A. 1999. Evolutionary genomics in
323 Metazoa: the mitochondrial DNA as a model system. *Gene* 238: 195-209.
- 324 Sambrook J, Fritsch EF, Maniatis T. 1989. *Molecular cloning: a laboratory manual*. Cold
325 spring harbor laboratory press.
- 326 Slatkin M, Barton NH. 1989. A comparison of three indirect methods for estimating
327 average levels of gene flow. *Evolution* 43: 1349-1368.
- 328 Suchard MA, Lemey P, Baele G, Ayres DL, Drummond AJ, Rambaut A. 2018. Bayesian
329 phylogenetic and phylodynamic data integration using BEAST 1.10. *Virus Evolution*
330 4: vey016.
- 331 Tajima F. 1989. Statistical method for testing the neutral mutation hypothesis by DNA
332 polymorphism. *Genetics* 123: 585-595.
- 333 Yang JQ, Hsu KC, Liu ZZ, Su LW, Kuo PH., Tang WQ, Zhou ZC, Liu D, Bao BL, Lin HD.
334 2016. The population history of *Garra orientalis* (Teleostei: Cyprinidae) using
335 mitochondrial DNA and microsatellite data with approximate Bayesian computation.
336 *BMC evolutionary biology* 16: 73.
- 337 Yeh FC, Yang RC, Boyle TB, Ye ZH, Mao JX. 1997. POPGENE, the user-friendly
338 shareware for population genetic analysis. *Molecular biology and biotechnology
339 centre, University of Alberta, Canada* 10: 295-301.
- 340 Zarza E, Reynoso VH, Emerson BC. 2011. Discordant patterns of geographic variation

341 between mitochondrial and microsatellite markers in the Mexican black iguana
342 (*Ctenosaura pectinata*) in a contact zone. *Journal of Biogeography* 38: 1394-1405.

343 Zhang W, LI YT, Jiang L. 2008. Fluvial process change of the typical multi-branched
344 meandering reach in the mid-down Yangtze River after three gorges dam
345 impoundment. *Journal of Sichuan University (Engineering Science Edition)* 40: 17-
346 24.

347 Zhuo Y, Hu H, Zhang L, Shu M. 2011. Microsatellite analysis of genetic diversity of
348 *Monopterus albus* along the middle and lower reaches of Yangtze River basin.
349 *Biotechnology Bulletin* 11: 187-192.

350

Figure 1

Figure 1. Sampling sites along the Yangtze River mapped using DIVA-GIS.

Three sampling sites from main stem included Wu Wei (WW), Gui Chi (GC) and Wang Jiang (WJ); three sampling sites from tributaries included Dang Tu (DT), Fan Chang (FC) and Huai Ning (HN). FC tributary connected to the main stem during the wet season and isolated during the dry season.

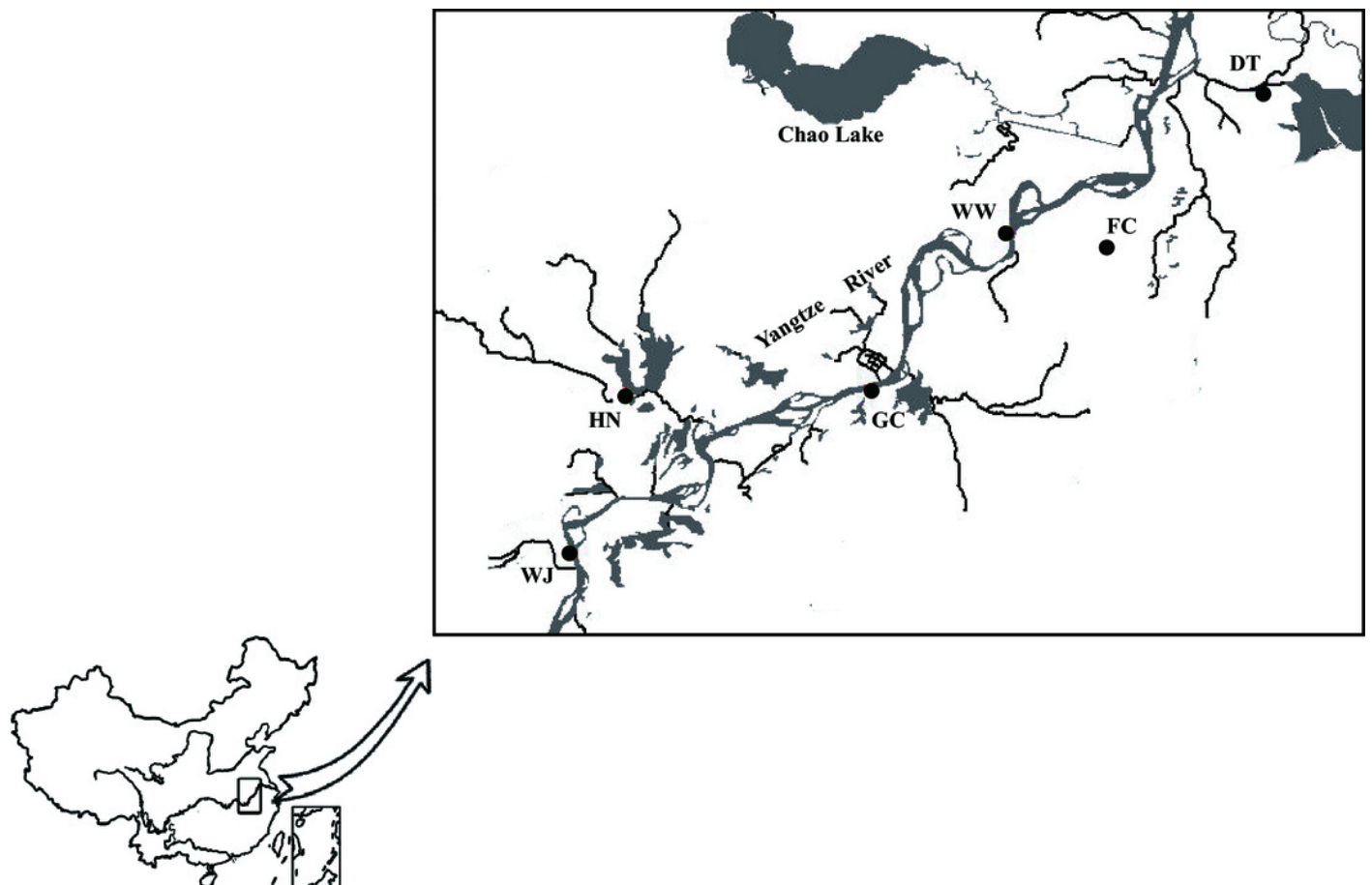


Figure 2

Figure 2. Haplotype network showing the genetic relationship of samples using MJ method.

Different colors represent the six populations. Circle size represents the number of sequences and numbers of nearby branches represent the mutation steps. The largest circle represents $n=24$ and the smallest circle represent $n=1$. Black dots represent mv.

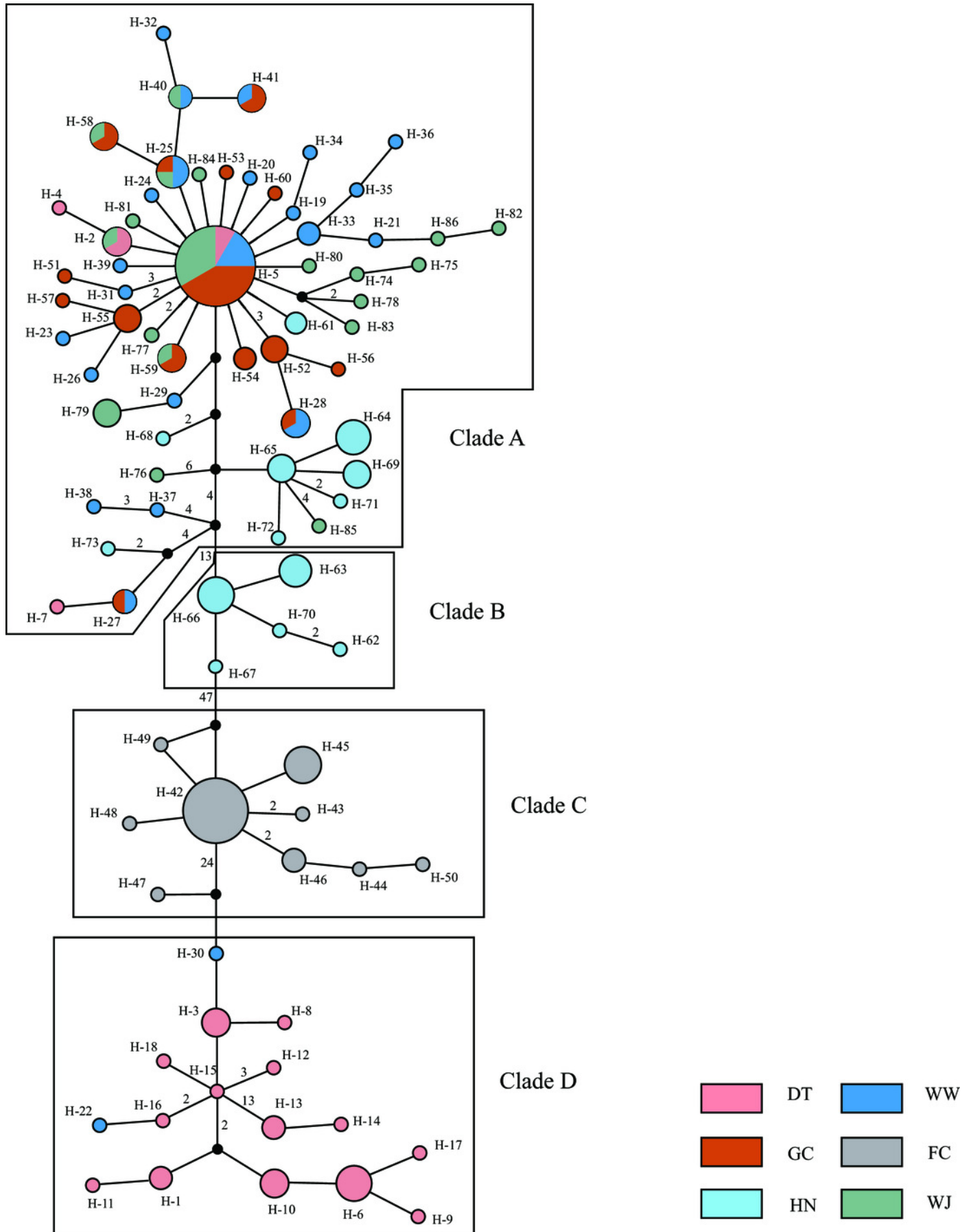


Figure 3

Figure 3. The demographic history inferred from mitochondrial data.

Samples from three main stem sampling sites were treated as one group. A: Mismatch distribution of main stem samples; B: Bayesian skyline plots of main stem samples, the shaded area represents the 95% confidence intervals of HPD analysis; C: Mismatch distribution of DT samples; D: Bayesian skyline plots of DT samples; E: Mismatch distribution of FC samples; F: Bayesian skyline plots of FC samples; G: Mismatch distribution of HN samples; H: Bayesian skyline plots of HN samples.

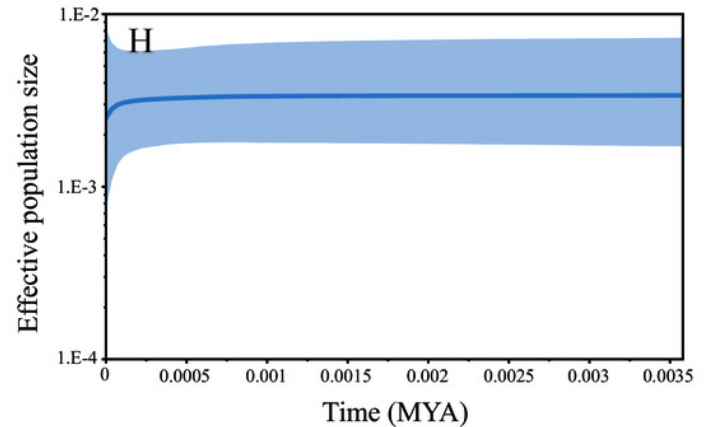
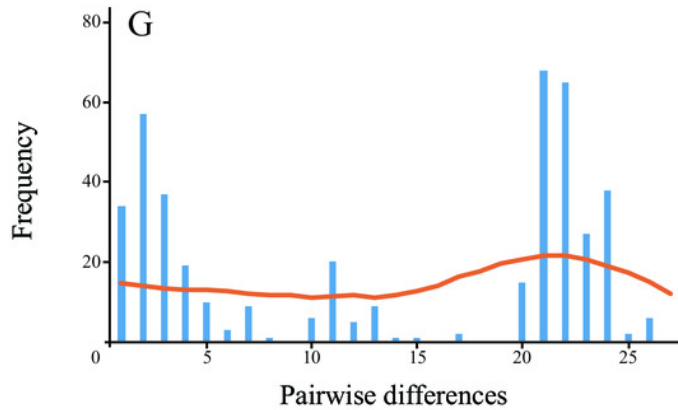
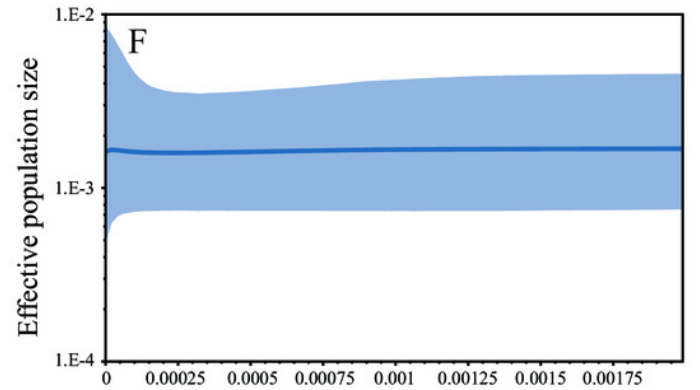
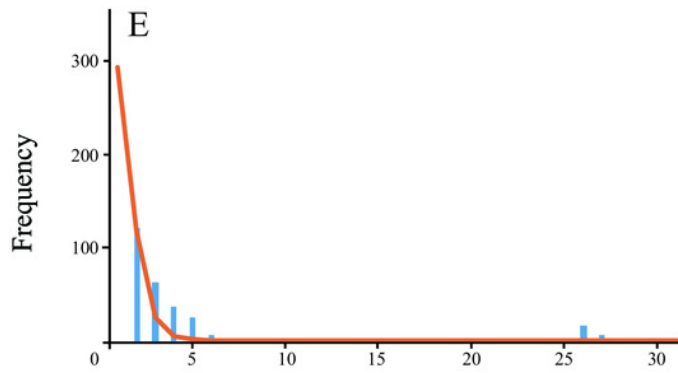
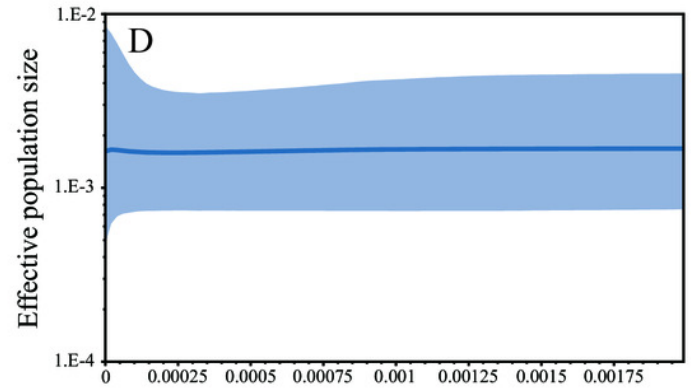
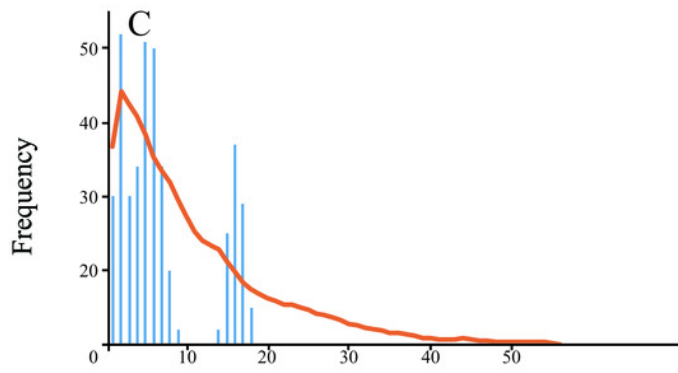
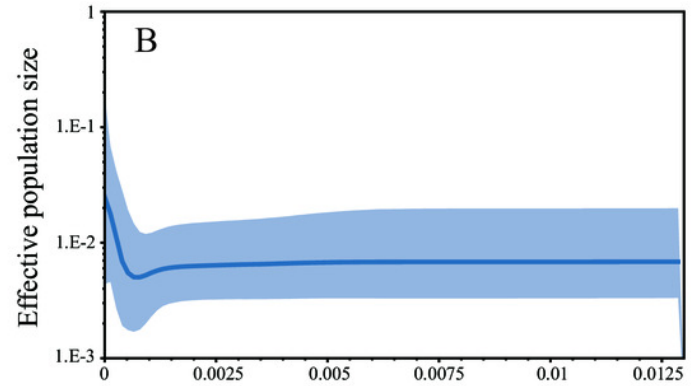
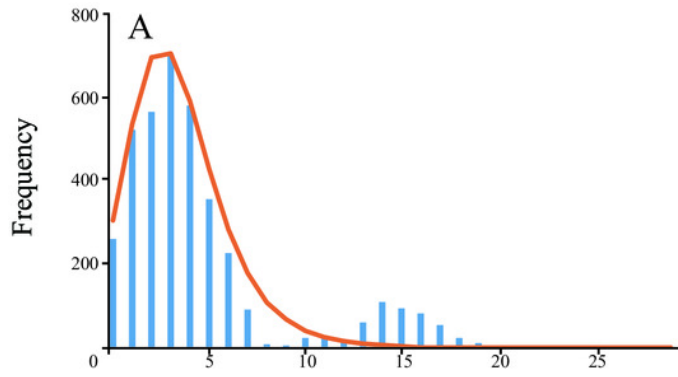


Figure 4

Figure 4. Population structure of 180 swamp eels showing for $K = 4$.

Four colors, e.g., red, yellow, purple and green, represent the inferred genetic clusters.

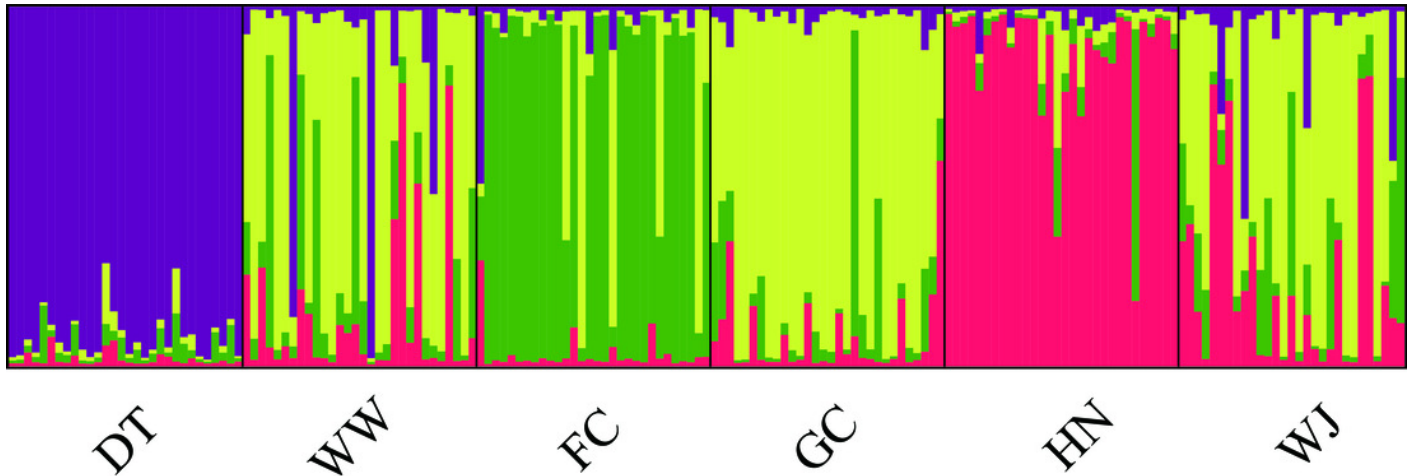


Figure 5

Figure 5. Plotmatrix indicating the correlation between genetic and geographic matrixes.

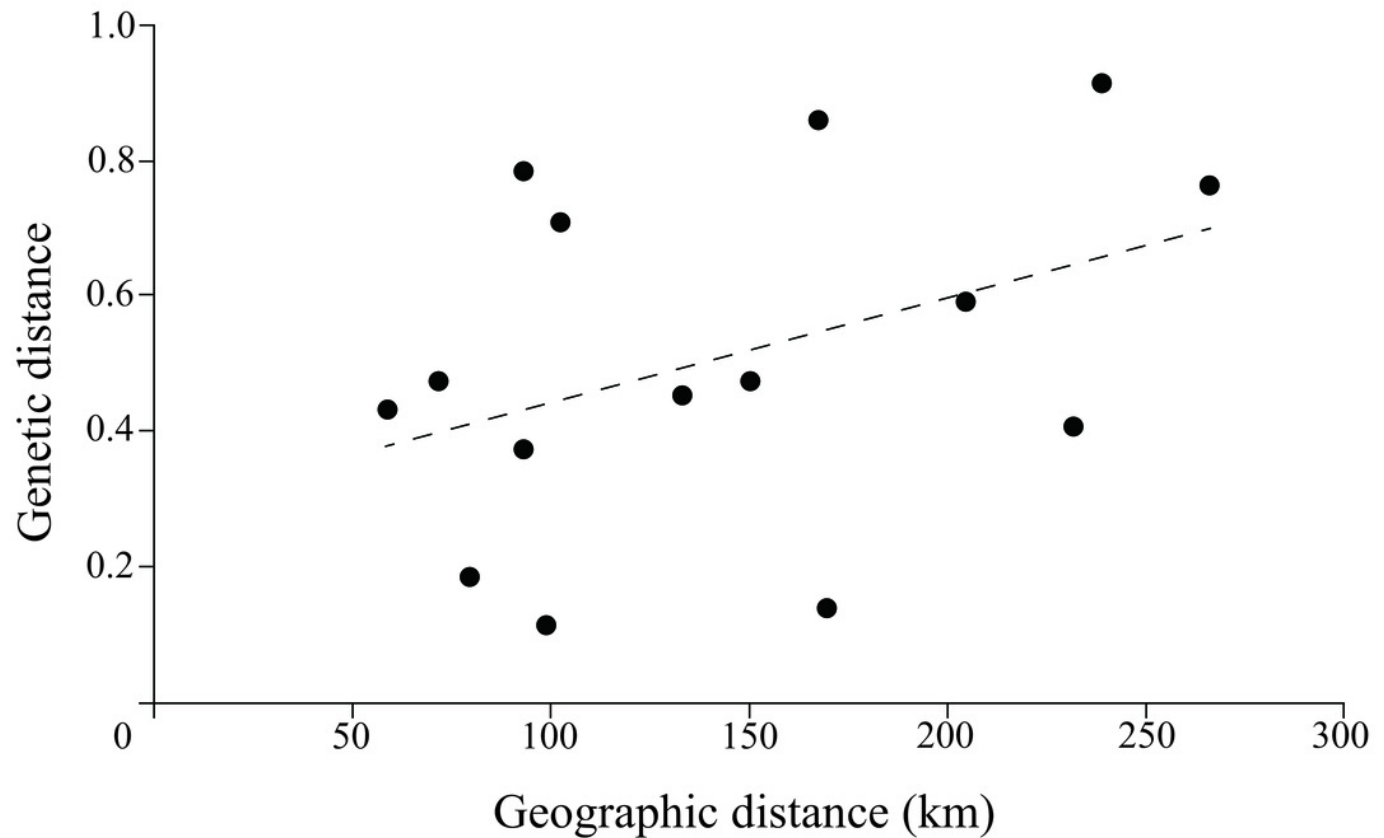


Figure 6

Figure 6. Diagram showing the unique life history and different hereditary patterns of mitochondrial DNA and nuclear DNA in sex reversal fish.

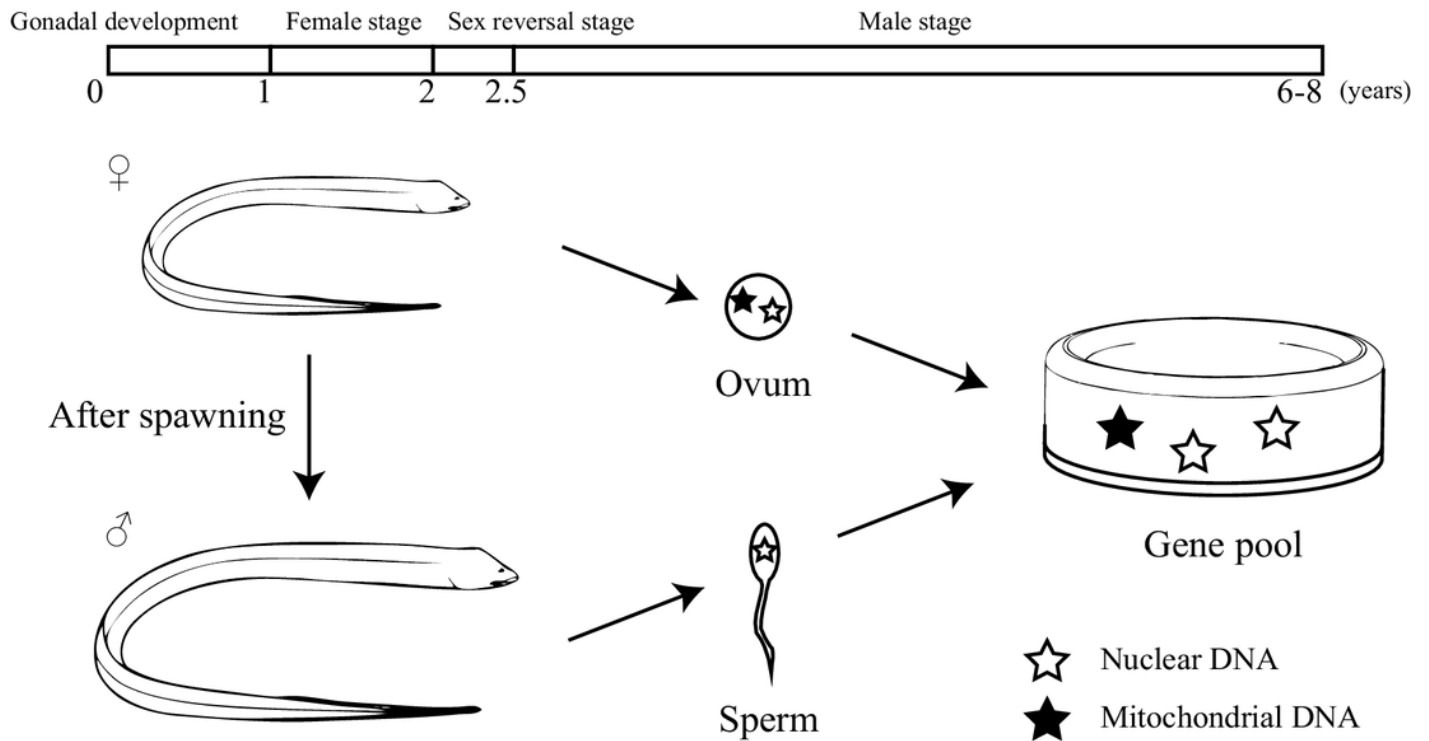


Table 1 (on next page)

Table 1. Genetic diversity of samples from six sites assessed using mitochondrial and microsatellite data

1

2

Table 1. Genetic diversity of samples from six sites assessed using mitochondrial and microsatellite data

Sampling sites	Mitochondrial genes			Microsatellite loci		
	Num. of haplotypes	<i>Hd</i>	<i>Pi</i>	Num. of alleles	<i>He</i>	<i>Ho</i>
DT (Tributary)	18	0.9540	0.0148	14	0.8749	0.7917
WW (main stem)	24	0.9793	0.0078	14	0.8638	0.7292
FC (Tributary)	9	0.6620	0.0017	12	0.8089	0.6542
GC (main stem)	15	0.8480	0.0021	13	0.8420	0.7417
HN (Tributary)	13	0.9220	0.0072	12	0.8052	0.5958
WJ (main stem)	19	0.9240	0.0023	14	0.8516	0.7802

3 *Hd* represents Haplotype diversity, *Pi* represents Nucleotide diversity, *He* represents Expected heterozygosity; *Ho* represents observed

4 heterozygosity

5

Table 2 (on next page)

Table 2 AMOVA of 6 sampling sites indicating the source of variation

1 **Table 2a. AMOVA of 6 sampling sites indicating the source of variation by mitochondrial data used**

Source of variation	df	Sum of squares	Percentage of variation	<i>P</i> value
Among sampling sites	5	1965.433	71.23	<0.001
Within sampling sites	174	908.533	28.77	<0.001
Total	179	2873.967		

2

3 **Table 2b. AMOVA of 6 sampling sites indicating the source of variation by microsatellite loci used**

Source of variation	df	Sum of squares	Percentage of variation	<i>P</i> value
Among sampling sites	5	76.325	5.35	<0.001
Within sampling sites	352	672.105	94.65	<0.001
total	357	1260.43		

4

5

Table 3 (on next page)

Table 3. Pairwise values of F_{st} (below diagonal) and P (above diagonal) between sampling sites

1 **Table 3a. Pairwise values of F_{st} (below diagonal) and P (above diagonal) between sampling sites estimated using**
 2 **mitochondrial data**

	DT	WW	FC	GC	HN	WJ
DT		<0.01	<0.01	<0.01	<0.01	<0.01
WW	0.6228		<0.01	0.08	<0.01	0.05
FC	0.5800	0.8510		<0.01	<0.01	<0.01
GC	0.7296	0.0242	0.9431		<0.01	<0.01
HN	0.6441	0.3069	0.8551	0.4750		<0.01
WJ	0.7253	0.0286	0.9391	0.0305	0.4594	

3 **Table 3b. Pairwise values of F_{st} (below diagonal) and P (above diagonal) between sampling sites estimated using**
 4 **microsatellite loci**

	DT	WW	FC	GC	HN	WJ
DT		<0.01	<0.01	<0.01	<0.01	<0.01
WW	0.0653		<0.01	0.06	<0.01	0.37
FC	0.0813	0.0509		<0.01	<0.01	<0.01
GC	0.0794	0.0077	0.0585		<0.01	0.63
HN	0.0982	0.0597	0.0869	0.0636		<0.01
WJ	0.0704	0.0030	0.0509	0.0005	0.0493	

6

Table 4 (on next page)

Table 4. Summary of neutrality and mismatch analyses indicating the demographic history

1

Table 4. Summary of neutrality and mismatch analyses indicating the demographic history

Populations	Tajima's D	Fu's F_s	τ	SSD (P)
Mainstream populations	-2.3328**	-24.9078**	2.2949	0.0056(0.36)
DT	0.6878	1.8735	0.3906	0.0034(0.53)
FC	-2.4163**	-0.8094	0.375	0.1446(0.02)
HN	0.4788	2.1653	22.5293	0.00496(0.008)

2 * $P < 0.05$; ** $P < 0.01$